UDC 629.78:629.785:539.4

SCIENTIFIC AND TECHNICAL ARTICLE

HYBRID METAL–COMPOSITE LOAD-CARRYING SHELL OF AN UPPER-STAGE CRYOGENIC TANK SECTION: PRELIMINARY ASSESSMENT OF THE ASPIRE R1 CONCEPT

Hybrid Metal–Composite Load-Carrying Shell for an Upper-Stage Cryogenic Tank: Preliminary Assessment of the ASPIRE R1 Concept

S. A. Sopov

Balkan Space Engineering Ltd, Varna, Bulgaria · Technical Director of the ASPIRE Reusable Transportation Space System Project

PUBLICATION STATUS

The dimensions, pressures and thicknesses presented are input data for the parametric study. They do not replace approved requirements, an analysis report, design documentation or authorisation for manufacture.

Abstract

The concept of a hybrid load-carrying shell for the cryogenic tank section of a launch-vehicle upper stage is considered. It combines a thin sealing liner made of an aluminium–lithium alloy, an adhesively bonded cellular core and an external carbon-fibre-reinforced polymer load-carrying shell. The purpose of the study is to determine the conditions for the fundamental feasibility of the architecture and to identify the parameters that must be confirmed before proceeding to detailed design. The analysis uses membrane theory of cylindrical shells, a compatible hoop-strain model for the metal and composite layers, estimates of axial compression and thermoelastic mismatch, and one-dimensional heat transfer. For the configuration studied, the hoop membrane resultant is 656 kN/m at an operating pressure of 0.32 MPa and 779 kN/m at a proof-level sensitivity of 0.38 MPa. A free 1.3 mm liner would experience approximately 505 and 599 MPa, respectively, making participation of the CFRP in carrying the hoop load mandatory. As the effective hoop modulus of the composite varies from 30 to 100 GPa, the calculated liner stress at operating pressure decreases from approximately 342 to 196 MPa. Cooling from 293 to 90 K creates a free strain mismatch of approximately 4.47×10^{-3}; edge zones, core terminations and transitions to load-bearing rings and domes therefore become governing. The thermal conductivity of the core is shown to dominate the through-thickness thermal resistance of the uniform panel. The concept is concluded to be potentially feasible, subject to combined analytical, process and experimental verification.

Keywords: cryogenic propellant tank; hybrid shell; aluminium–lithium alloy; CFRP; honeycomb core; bonded joint; thermoelasticity; buckling; friction stir welding.

Abstract

A hybrid load-carrying shell is investigated for an upper-stage cryogenic propellant-tank section. The architecture combines a thin aluminium–lithium sealing liner, a bonded cellular core and an external carbon-fibre-reinforced polymer (CFRP) shell. The study aims to identify feasibility conditions and the parameters that must be verified before detailed design. Thin-shell membrane theory, a compatible-strain metal/CFRP load-sharing model, axial-compression screening, thermoelastic-mismatch estimates and one-dimensional heat-transfer sensitivity are applied. For the study configuration, the circumferential membrane resultant is 656 kN/m at 0.32 MPa and 779 kN/m at 0.38 MPa. A free 1.3 mm liner would develop approximately 505 and 599 MPa, respectively; circumferential CFRP reinforcement is therefore mandatory. Increasing the effective hoop modulus of the laminate from 30 to 100 GPa reduces the calculated liner stress at operating pressure from about 342 to 196 MPa. Cooling from 293 to 90 K produces a free mismatch strain of approximately 4.47×10^{-3}, making terminations, ring interfaces and dome transitions more critical than the uniform barrel. The cellular core is shown to dominate the through-thickness thermal resistance of the idealised panel. The concept is potentially feasible, but only after coupled nonlinear analysis, process qualification and a building-block test programme.

Keywords: cryogenic propellant tank; hybrid shell; aluminium–lithium alloy; CFRP; cellular core; bonded joint; thermoelastic mismatch; buckling.

1. Introduction

The mass of an upper-stage tank section directly affects launch-vehicle performance; however, reducing it is simultaneously constrained by strength, stability, leak-tightness, thermal conditions and large-scale manufacturing technology. Conventional metallic tanks provide proven leak-tightness and repairability, but further reduction of shell thickness rapidly increases sensitivity to buckling, weld defects and geometric imperfections. Fully composite cryogenic tanks promise significant mass reduction, but impose stringent requirements on matrix resistance to microcracking, permeability and the quality of highly loaded transition joints.

Experience from the X-33 programme showed that microcracks in the inner composite skin and ingress of cryogenic fluid into the honeycomb core can create a hazardous damage mechanism during subsequent warm-up [1]. At the same time, NASA's Composite Cryotank Technologies and Demonstration programme confirmed that large-scale composite tanks can be manufactured and cryogenically tested, but also demonstrated the governing role of transition Y-joints, local thermal stresses and staged experimental development [2]. Analytical studies of composite cryotanks likewise emphasise the need to combine laminate mechanics with progressive-damage and durability analysis [8]. Thus, the transition to composites does not eliminate the problem of leak-tightness and joints; it transfers it into another form.

This paper considers an intermediate architecture: the metallic liner provides leak-tightness and local damage tolerance; the external CFRP shell carries a specified share of the membrane load; and the cellular core stabilises the thin layers, transfers interlaminar shear and provides through-thickness thermal resistance. The methodological objective is not to demonstrate the readiness of a specific tank, but to construct a reproducible parametric assessment linking pressure, composite hoop stiffness, thermoelastic mismatch and core properties.

The objective of the study is to determine the conditions required for feasibility of the hybrid shell as applied to the ASPIRE R1 concept and to formulate a verification route enabling progression from first-order calculations to a qualified design.

2. Object of Study and Analysis Assumptions

The cylindrical region of a cryogenic tank section is studied. The parameters in Table 1 are used as a single set of input data for the sensitivity analysis. They are candidate values and shall not be interpreted as final design requirements.

Table 1 — Input data for the parametric study

Parameter	Value adopted in the study	Purpose
Outer cylinder diameter	4.10 m	Geometric scale
Al–Li liner thickness	1.30 mm	Candidate sealing shell
Outer CFRP shell thickness	1.50 mm	Single value for stiffness assessment
Cellular core height	20 mm	Stabilisation, shear, thermal resistance
Thickness of each adhesive layer	0.50 mm	Parameter of the one-dimensional thermal model
Operating pressure	0.32 MPa	Membrane assessment
Proof-level sensitivity	0.38 MPa	Does not replace the specified proof requirement
Axial compression	1.6 MN	Screening, non-limit load case
Temperatures	293 / 111 / 90 K	Ambient / LCH_4 / LOX level

Note: material properties, the CFRP lay-up, cell geometry, welds and safety factors have not been fixed at this stage.

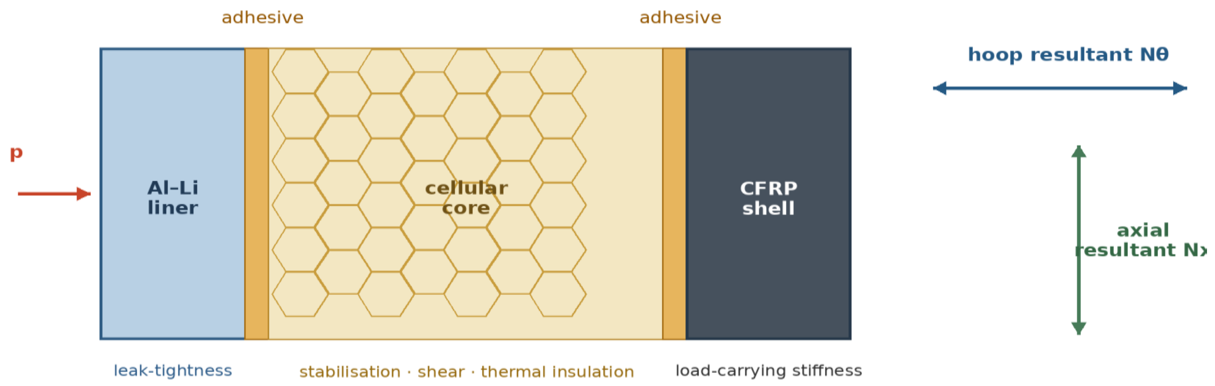

Figure 1 — Functional separation of the layers and principal load-transfer paths

The viability of the architecture is governed not by the strength of the individual materials, but by closure of the load-transfer path. Pressure creates a hoop membrane resultant that must be redistributed between the liner and the CFRP through the bonded, core-filled interface. Axial loads are transferred through the longitudinal stiffness of the composite shell and through the ring and dome transitions. Interlaminar shear and peel stresses arise in the edge zones and are absent from the model of an infinitely long uniform panel.

3. Preliminary Assessment Methodology

3.1. Membrane Load from Internal Pressure

For a thin cylindrical shell, the hoop resultant per unit axial length is determined by

$$N\theta = pD / 2 \tag{1}$$

and the stress in a free metallic liner is given by

$$\sigma\theta{,}free = N\theta / tAl = pD / (2tAl). \tag{2}$$

These relationships establish the required load-carrying level, but do not account for local bending, welds, ovality, cut-outs, damage or knockdown factors applied to allowable properties.

3.2. Load Sharing between Metal and CFRP

For a long, uniformly bonded region, compatibility of the hoop strains in the metallic and composite layers is assumed. To a first approximation, the load share remaining in the liner and the corresponding stress are

$$f_{Al} = E_{Al} t_{Al} / (E_{Al} t_{Al} + E_{\theta,CFRP} t_{CFRP}); \quad \sigma_{Al} = f_{Al} N_\theta / t_{Al}. \tag{3}$$

Here $E_{\theta,CFRP}$ is the effective hoop modulus of the actual multilayer lay-up. For illustration, E_{Al} = 73 GPa is adopted. Equation (3) is applicable only to the uniform region and does not describe shear-lag at edges, core terminations, seams, inserts or load-bearing rings.

3.3. Axial Compression and Stability

The average axial membrane resultant for the screening load F_x is determined as

$$N_x = F_x / (\pi D). \tag{4}$$

For a thin-walled shell, material strength is not a sufficient criterion. The design critical load must be obtained from a nonlinear model including geometric imperfections and confirmed by testing. In general form, the condition may be written as

$$N_{cr,design} = KDF \cdot N_{cr,perfect} / \gamma \geq N_x, \tag{5}$$

where KDF is the validated knockdown factor for imperfections and γ is the design factor. NASA SP-8007-2020/Rev. 2 provides methodological guidance for assessing the imperfection sensitivity of cylindrical shells, but does not replace the requirements of a specific programme [3]. For a sandwich wall, global buckling, intracell dimpling, core crushing and shear, wrinkling of the outer face and adhesive-joint debonding are additionally checked.

3.4. Thermoelastic Mismatch

The free difference between the thermal strains of the metal and CFRP is estimated as

$$\Delta\varepsilon_{free} = (\alpha_{Al} - \alpha_{CFRP}) \Delta T. \tag{6}$$

For the screening estimate, $\alpha_{Al} = 22 \cdot 10^{-6}$ K^{-1} and a near-zero effective CFRP value in the direction considered are adopted. If a relative displacement δ is transferred through a core of height h_{core}, its nominal shear strain is

$$\gamma_{core} = \delta / h_{core}. \tag{7}$$

Equation (7) indicates the kinematic trend, but does not permit a direct assertion that stresses decrease by the same amount as core height increases: the actual field depends on shear modulus, load-transfer length, adhesive nonlinearity and edge restraints.

3.5. Heat Transfer through a Uniform Panel

For a series one-dimensional approximation, the total thermal resistance and steady-state heat flux are

$$R_{total} = \Sigma(t_i / k_i) + \Sigma R_{contact}; \quad q = \Delta T / R_{total}. \tag{8}$$

The values used are k_{Al} = 100 W/(m·K), through-thickness k_{CFRP} = 0.5 W/(m·K), k_{adh} = 0.2 W/(m·K), and ΔT = 203 K. The effective thermal conductivity of the core is varied from 0.05 to 0.50 W/(m·K). Contact resistances, radiative exchange within the cells, external insulation and local thermal bridges are not included in this model.

4. Results and Discussion

4.1. Need for Hoop Reinforcement

At the operating pressure of 0.32 MPa, the hoop membrane resultant is 656 kN/m, and at 0.38 MPa it is 779 kN/m. If this load is carried only by the 1.3 mm liner, the calculated stresses reach 505 and 599 MPa, respectively. These values represent load demand, not a strength margin. They show that the thin liner cannot be regarded as an independent load-carrying shell.

Table 2 — Sensitivity of liner loading to CFRP hoop stiffness

$E_{\theta,CFRP}$, GPa	Load share in Al	σ_{Al} at 0.32 MPa	σ_{Al} at 0.38 MPa

Eθ,CFRP, GPa	Load share in Al	σAl at 0.32 MPa	σAl at 0.38 MPa
10	86.4%	436 MPa	517 MPa
30	67.8%	342 MPa	406 MPa
60	51.3%	259 MPa	308 MPa
100	38.8%	196 MPa	232 MPa

Calculated from strain compatibility; does not account for edge shear-lag and does not establish an allowable stress.

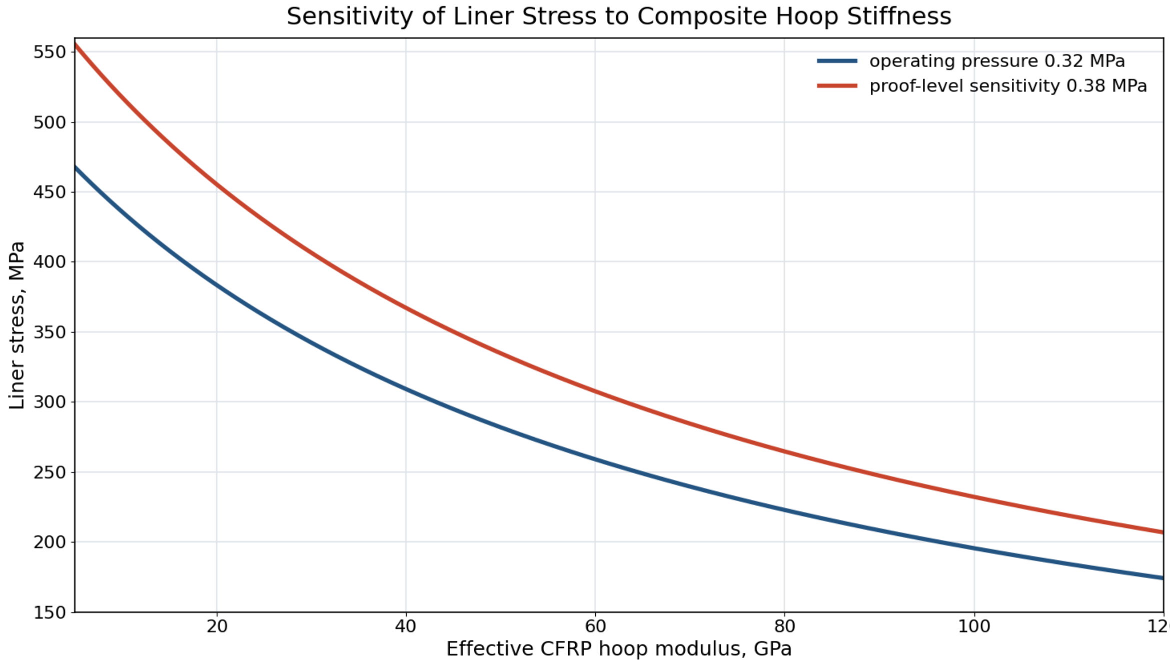

Figure 2 — Effect of the effective CFRP hoop modulus on stress in the metallic liner

The result establishes a fundamental lay-up requirement: a predominance of longitudinal fibres alone is insufficient. A measurable hoop stiffness is required, and the laminate ABD matrix must be defined together with strength and microcracking constraints. Bonding and shear-lag must be modelled in transition regions, because local peel failure may occur even when the average liner stress is acceptable.

4.2. Axial Compression and Buckling

For Fx = 1.6 MN, Equation (4) gives Nx ≈ 124.2 kN/m. If the entire load is notionally assigned only to the 1.5 mm CFRP layer, the average compressive stress is approximately 82.8 MPa. For a thin cylindrical shell, however, this value does not determine viability: global and local stability are generally more sensitive to panel length, ring restraint, ovality, dents, layer misalignment and internal pressure. Cell size and core height must therefore be selected not from a single equation, but through multi-criteria optimisation of “mass — stability — interlaminar stresses — heat transfer — manufacturability”.

4.3. Thermoelastic Compatibility

Cooling from 293 to 90 K creates a free strain mismatch of approximately $4.47 \cdot 10^{-3}$, or 4,470 μm/m. This is equivalent to a free relative displacement of 4.47 mm per metre of length. At 111 K, the estimate is approximately 4,000 μm/m. In a uniform infinite region, compatibility can redistribute strains between the layers; however, concentrated shear and peel stresses develop at free edges, seams, cut-outs, and transitions to domes and rings.

Increasing the core height from 11.5 to 20 mm at the same local displacement reduces the nominal shear strain to 57.5% of its original value, i.e. by 42.5%. This effect is beneficial, but cannot automatically be applied to stress and service life: mass, local stability, thermal bridges and sensitivity to bonding defects change at the same time.

4.4. Thermal Sensitivity

Table 3 — Sensitivity of heat transfer through a uniform panel

Core keff, W/(m·K)	Rtotal, m²·K/W	q, W/m²	ΔT across the two adhesive layers
0.05	0.4080	498	2.5 K
0.10	0.2080	976	4.9 K
0.20	0.1080	1 879	9.4 K
0.50	0.0480	4 228	21.1 K

Steady-state estimate for ΔT = 203 K. The values are not a prediction of the total heat leak into the tank.

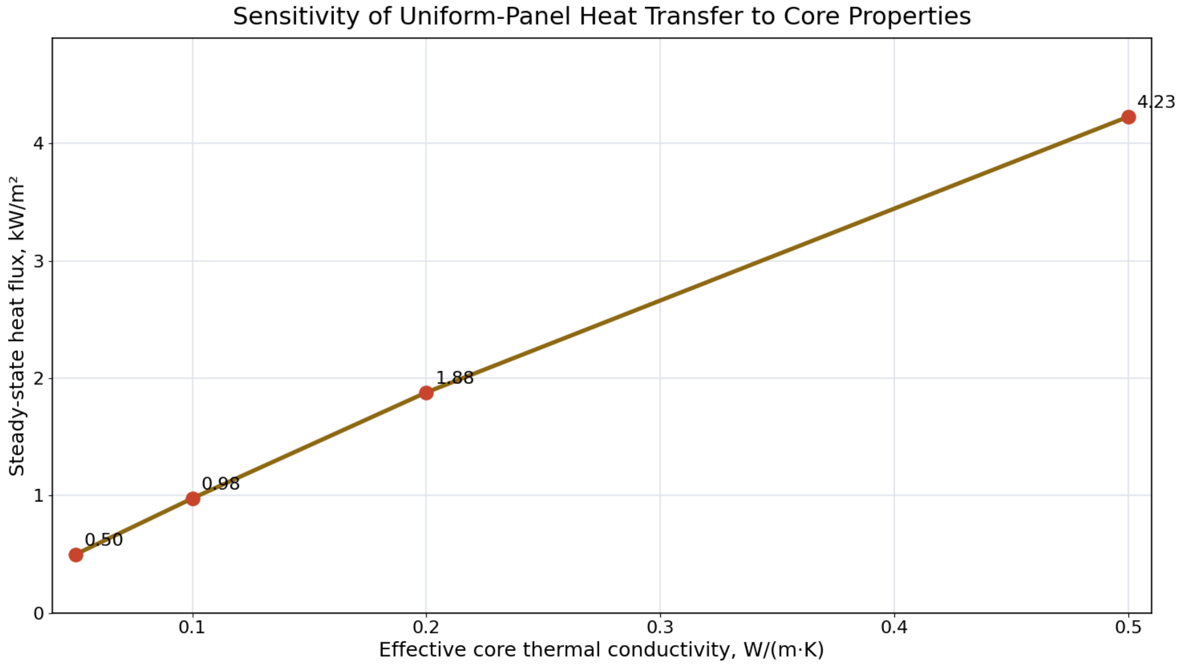

Figure 3 — Effect of effective core thermal conductivity on heat flux through a uniform panel

In the adopted model, the core makes the principal contribution to thermal resistance. Its material, cell orientation, density, radiative exchange and the state of the gas inside the cells are therefore governing rather than secondary parameters. The share of the adhesive layers in the total temperature drop is relatively small in the uniform region; however, two-dimensional thermal bridges near metallic inserts, core terminations and rings can sharply alter the local temperature and stress fields. Design therefore requires a transient coupled model, rather than a steady-state one-dimensional model, with separate cooling, dwell, draining and warm-up regimes.

4.5. Materials, Welding and Transition Joints

Al–Li 2195 is technologically attractive because of its reduced density, high specific strength and heritage in cryogenic structures. NASA and industry have developed friction stir welding (FSW) of this alloy for large tanks [4, 5]. However, published studies predominantly concern sheets and plates thicker than the candidate 1.3 mm liner; transferring that manufacturing heritage to an ultra-thin shell without separate qualification is unacceptable.

Forming large domes from 2195 also requires microstructural control. During heat treatment of FSW blanks after forming, abnormal grain growth has been observed that can impair ductility and fracture resistance; NASA investigated an intermediate anneal as a means of reducing this risk [6]. Separate studies of stretch forming of gores confirmed that acceptable properties are achieved only through a coordinated selection of heat treatment and deformation process [7]. Consequently, the route “blank — welding — forming — heat treatment” must be qualified as a single process.

The adhesive cannot be selected solely on the basis of room-temperature strength. Data are required for shear and Mode I/II fracture at 293, 111 and 90 K; residual strength after cooling cycles; oxygen and methane compatibility; moisture uptake; creep; bondline-thickness control; surface preparation; repairability; and probability of defect detection. The cure temperature must be compatible with the Al–Li temper, the CFRP cycle and the allowable residual stresses.

5. System-Level Assessment of the Concept

The hybrid shell occupies an intermediate position between a metallic tank and an all-composite tank. Its potential advantage does not arise from mechanically adding three materials, but from functional separation: the metal provides leak-tightness, the composite provides high specific stiffness, and the core provides stability and thermal resistance. This advantage arises only when load is transferred reliably through the interface.

Table 4 — Advantages, risks and implementation conditions

Potential advantage	Critical risk	Required confirmation
Reduced mass of the load-carrying wall	The mass of adhesive, core, rings and reinforcements consumes the gain	Complete mass roll-up including manufacturing and design margins
Leak-tightness of the metallic liner	High stresses and damage susceptibility of the thin shell	Combined loading with CFRP, fracture control, proof/leak test
High CFRP hoop stiffness	Microcracking, delamination and impact damage	Allowables, NDI, damage tolerance and cryogenic testing
Thermal resistance of the core	Thermal bridges and gas in the cells	2D/3D transient thermal model and panel test
Integration of functions in a single wall	Complex manufacturing and repair	Technology demonstrator and defect map

The greatest structural risk is concentrated not in the middle of the cylindrical panel, but at layer terminations and stiffness transitions. Ring elements, dome transitions, nozzles, welds, line attachments and manufacturing cut-outs create a three-dimensional stress state. These zones must determine the architecture of the test articles and the verification sequence.

For an expendable upper stage, multi-flight life is not an initial requirement; nevertheless, the structure still undergoes manufacturing, acceptance, fuelling, cooling, draining and pre-launch cycles. Qualification must therefore combine strength and leak-tightness verification with a damage-tolerance approach and residual-strength analysis after the specified event spectrum.

6. Recommended Verification Programme

A rational technical-risk reduction route follows the building-block approach successfully applied in large composite cryotank programmes [2]. Each subsequent level should begin only after the analytical model has been correlated with the results of the preceding level.

Table 5 — Staged analytical and experimental verification programme

Level	Test article	Main tasks	Gate criterion
1. Material	Al/adhesive/core/CFRP coupons	Shear, Mode I/II, CTE, k, cycles 293↔111/90 K, compatibility	Statistical allowables and selected process
2. Element	Flat and curved sandwich panel	Dimpling, wrinkling, core shear, NDI, bond defects	Correlation of local FEM and allowable defects
3. Transition	Ring/dome, core termination, FSW seam with overwrap	Shear-lag, peel, thermal bridge, manufacturing tolerances	Validated 3D model and repair process

Level	Test article	Main tasks	Gate criterion
4. Subscale	Cylinder or tank demonstrator	Cooling, pressure, combined load, leak/NDI	Proof without degradation; predictable failure
5. Full tank	Qualification article	Proof, burst, cycles, leak-tightness, post-test inspection	Closed requirements and approved design justification

In parallel with testing, two linked models must be developed: a global shell model of the tank and local solid/cohesive models of the transitions. The temperature field must be transferred into the structural analysis, while measured geometric imperfections and joint properties must be used instead of nominal values. This approach reduces the risk of late discovery that a ring joint or adhesive interface is unworkable.

7. Study Limitations

The results obtained are preliminary. The study does not include an approved CFRP lay-up, cryogenic material allowables, the actual cell and cell-wall geometry, a nonlinear adhesive model, weld knockdown factors, measured imperfections, a combined load matrix or experimental correlation. The one-dimensional thermal model does not account for radiation, convection, external insulation or local bridges. The stresses and heat fluxes presented are therefore not design margins or operating characteristics of the product.

8. Conclusions

1. The hybrid architecture “Al–Li liner — cellular core — CFRP shell” is potentially feasible if the layers are designed as a single load-carrying system rather than as independent shells.
2. At a diameter of 4.10 m and a pressure of 0.32 MPa, the hoop resultant is 656 kN/m. A free 1.3 mm liner would develop approximately 505 MPa; therefore, CFRP hoop stiffness and demonstrated load transfer are mandatory.
3. As the effective CFRP hoop modulus increases from 30 to 100 GPa, the calculated liner stress at operating pressure decreases from approximately 342 to 196 MPa. This confirms the need to finalise the laminate lay-up together with the strength of the liner and interface.
4. The free thermoelastic mismatch during cooling from 293 to 90 K reaches approximately 4,470 µm/m. Layer terminations, ring elements, dome transitions, seams and cut-outs become critical.
5. The cellular core governs not only stability, but also the principal share of through-thickness thermal resistance. Its properties must be specified through joint optimisation of mass, heat transfer, shear-lag and manufacturability.
6. The next stage must include selection of materials and lay-up, nonlinear analysis with imperfections, a transient thermomechanical model, and a coupon → element → transition → subscale tank → qualification tank programme.

References

1. Grimsley B. W., Cano R. J., Johnston N. J., Loos A. C., McMahon W. M. Hybrid Composites for LH2 Fuel Tank Structure. NASA Technical Reports Server, Document ID 20040086019, 2004. https://ntrs.nasa.gov/citations/20040086019

2. Jackson J. R., Vickers J., Fikes J. Composite Cryotank Technologies and Development: 2.4 and 5.5 m Out-of-Autoclave Tank Test Results. NASA Technical Reports Server, Document ID 20150021410, 2015. https://ntrs.nasa.gov/citations/20150021410

3. Hilburger M. W. Buckling of Thin-Walled Circular Cylinders. NASA/SP-8007-2020/REV 2. NASA Langley Research Center, 2020; updated issue 2023. https://ntrs.nasa.gov/citations/20205011530

4. Loftus Z., Arbegast W. J., Hartley P. J. Friction Stir Weld Tooling Development for Application on the 2195 Al-Cu-Li Space Transportation System External Tank. NASA/CR-1998-208260, 1998. https://ntrs.nasa.gov/citations/19980201001

5. Kinchen D. G., Li Z., Adams G. P. Mechanical Properties of Friction Stir Welds in Al 2195-T8. NASA Technical Reports Server, Document ID 19990064489, 1999. https://ntrs.nasa.gov/citations/19990064489

6. Hales S. J., Tayon W. A., Domack M. S. Friction-Stir-Welded and Spin-Formed End Domes for Cryogenic Tanks. JANNAF Annual Meeting, 2012. NASA NTRS Document ID 20120008817. https://ntrs.nasa.gov/citations/20120008817

7. Volz M. P., Chen P. S., Gorti S., Salvail P. Development of Aluminum-Lithium 2195 Gores by the Stretch Forming Process. NASA Technical Reports Server, Document ID 20140011717, 2014. https://ntrs.nasa.gov/citations/20140011717

8. Abumen G. H., Kosareo D. N., Roche J. M. Cryogenic Composite Tank Design for Next Generation Launch Technology. 40th AIAA/ASME/SAE/ASEE Joint Propulsion Conference, 2004. NASA NTRS Document ID 20050051705. https://ntrs.nasa.gov/citations/20050051705

Author Information

Sergey Alekseevich Sopov — radio-electronics engineer; Technical Director of the ASPIRE Reusable Transportation Space System Project; Balkan Space Engineering Ltd, Varna, Bulgaria.